

Contents

1 Article Information	1
2 Motivation and Problem Addressed	1
3 DFT Calculations and Thermochemistry Modeling	2
4 Highlights of Results	4
5 Critical Review	5

1 Article Information

The article reviewed in this report is the following:

Zhang, B., Duan, Y., Johnson, K. *Density functional theory study of CO₂ capture with transition metal oxides and hydroxides*. (2012) **The Journal of Chemical Physics**, 136(6):064516.

This report is organized as follows. Section [2](#) motivates and defines the objectives of the problem addressed in the article. Section [3](#) summarizes the authors' approach to performing DFT calculations and modeling the thermochemistry of the CO₂ capture. Section [4](#) highlights some of the results obtained. Finally, section [5](#) presents a critical review of the methodology and results.

2 Motivation and Problem Addressed

Carbon dioxide (CO₂) is one of the primary greenhouse gases. Therefore, researchers have investigated efficient ways to capture and sequester CO₂ in order to mitigate its effect on global climate change. There are three classes of CO₂ capture technologies:

- **Pre-combustion:** Removal of CO₂ from the fossil fuel prior to combustion
- **Post-combustion:** CO₂ capture from the flue gas after combustion of the fossil fuel (traditionally scrubbing with liquid monoethanolamine (MEA))
- **Oxy-fuel:** Combustion of fossil fuel with pure oxygen rather than air (avoids NO_x and concentrates CO₂)

The main objectives of the article are as follows:

- Investigate the efficiency of solid sorbents to capture CO₂;
- Compute phase diagrams of reactions between sorbents and CO₂;

- Assess the accuracy of five different Density Functional Theory (DFT) generalized gradient functionals for the prediction of the reaction thermodynamics of various transition metal oxides and hydroxides;
- Screen these materials for suitability in pre-combustion and post-combustion CO₂ capture.

3 DFT Calculations and Thermochemistry Modeling

Two computational packages were employed to perform the DFT calculations: VASP and GPAW. Functionals were used to calculate the ground state energies of all the solid phase and gas phase compounds. Table 1 gives the details of the features used in each package. The k -point meshes generated for both packages were generated with a spacing of around 0.027 \AA^{-1} between k -points along the axes of the reciprocal unit cells.

Table 1: Features of each computational package.

Feature	VASP	GPAW
CE Interactions	PAW potentials	–
XC Potentials	PW91 (CG), PBEsol (QN)	PBE, TPSS, revTPSS
Energy convergence	0.01 meV	10^{-6} eV/atom , grid spacing of 0.15 \AA
Energy cut-off	520 eV	–
k -point meshes	Monkhorst-Pack	Monkhorst-Pack

where CE stands for core-electron, XC stands for exchange-correlation, PAW stands for Projector Augmented-Wave, CG stands for conjugate-gradient method, QN stands for quasi-Newton method.

The thermochemistry for the CO₂ capture reactions was modeled using statistical mechanics ideal gas expressions. The temperature-related free energy of gas species is given by:

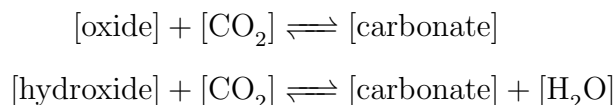
$$G^0 = U + PV - TS \approx U_{\text{DFT}} + U_{\text{ZPE}} + U_{\text{trans+rot}}(T) + U_{\text{vib}}(T) + PV - TS(T) \quad (1)$$

where U_{DFT} is the electronic total energy of the material as computed using DFT, U_{ZPE} is the zero point energy (ZPE) of the gas, and

$$\begin{aligned}
 U_{\text{trans+rot}}(T) &= \begin{cases} \frac{5}{2}RT & \text{for linear molecules} \\ \frac{6}{2}RT & \text{for nonlinear molecules} \end{cases} \\
 U_{\text{vib}}(T) &= \sum_i \frac{R\theta_i}{\exp(\theta_i/T) - 1} \\
 S(T) &= A \ln(t) + Bt + \frac{Ct^2}{2} + \frac{Dt^3}{3} - \frac{E}{2t^2} + F
 \end{aligned}$$

where $t = T/1000$ and parameters (A , B , C , D , E , F) are taken from NIST chemistry webbook (Shomate Equation).

The reactions are expressed in the following general way:



Thus, the free energy change of reaction is calculated by:

$$\Delta G = \Delta G_{\text{solid}} + \Delta G_{\text{CO}_2} \quad (2)$$

or

$$\Delta G = \Delta G_{\text{solid}} + \Delta G_{\text{CO}_2} - \Delta G_{\text{H}_2\text{O}} \quad (3)$$

for reactions without and with water, respectively.

Since the volume change due to gas generation is very large relative to the volume change of solid materials, we can neglect the volume change of solid phases without significant loss of accuracy. If the activities of all solid components are taken to be 1, the equilibrium pressure of the overall reaction can then be written as:

$$\frac{P_{\text{CO}_2}}{P_0} = \exp\left(-\frac{\Delta G}{RT}\right) \quad (4)$$

where P_0 is the standard state pressure (1 bar), or

$$\frac{P_{\text{CO}_2}}{P_{\text{H}_2\text{O}}} = \exp\left(-\frac{\Delta G}{RT}\right) \quad (5)$$

for reactions without and with H_2O , respectively. The van't Hoff plots are obtained by plotting the equilibrium pressures from equations (4) or (5) as a function of the inverse absolute temperature.

Phase diagrams for the solids were obtained by minimizing the grand-canonical Gibbs free energy of a system where all possible solid phases are in contact with a gas-phase reservoir having specified partial pressures of CO_2 and H_2O . Hence, the optimization problem solved is to minimize

$$G(T, \mu_{\text{gas}}) = \sum_{j=1}^S x^j F^j(T) - \sum_k \sum_{j=1}^S \mu_k^{\text{gas}}(T, p) x_k^{j, \text{gas}} \quad (6)$$

subject to (mass conservation constraint):

$$\sum_{i=\text{metal}}^M f_i = \sum_{i=\text{metal}}^M \sum_{j=1}^S x^{j, \text{solid}} b_i^{j, \text{solid}} = 1 \quad (7)$$

where $F^j(T)$ is the free energy of solid phase j (ignoring the pV term contribution), S is the number of solid substances, $\mu_k^{\text{gas}}(T, p)$ is the chemical potential of gas species k (CO_2 and H_2O), x^j is the unknown mole fraction of phase j coexisting at a given composition, temperature, and pressure, $x_k^{j, \text{gas}}$ is the theoretical mole fraction of gas species k contained

in phase j , f_i is the molar ratio of solid element i in all solids, $b_i^{j,\text{solid}}$ represents the number of atoms of type i in one formula unit of phase j , and M is the number of elements.

The authors chose sufficiently small intervals of temperature and pressure to ensure adequately small chemical potential changes between two steps in order to guarantee single step reactions.

4 Highlights of Results

Figure 1 shows partial results for the DFT calculations. It can be noted that better agreement with experimental values of lattice parameters were obtained when using PBEsol for compounds containing Zn and Cd except $\text{Zn}(\text{OH})_2$ and using PW91 for compounds containing Mn and Ni. Regarding entropies calculated from frozen-phonon approach, discrepancies are within 10 J/(mol K) except for NiO and $\text{Ni}(\text{OH})_2$.

Compound	Space group	Lattice parameters ^a			Enthalpy of formation ^b (kJ/mol)			Entropy ^c (J/mol K)	
		Expt.	PW91	PBEsol	Expt.	PW91	PBEsol	Expt.	PW91
MnO	$Fm\bar{3}m$	a = 4.446	a = 4.3281	a = 4.3367	− 385.2	− 246.1	− 231.4	59.71	49.98
NiO	$Fm\bar{3}m$	a = 4.1944	a = 4.1809	a = 4.1056	− 239.7	− 103.7	− 108.2	37.99	53.75
ZnO	$P6_3mc$	a = 3.2525	a = 3.2806	a = 3.2389	− 350.5	− 289.7	− 288.4	43.64	45.31
		c = 5.2111	c = 5.2978	c = 5.2276					
		$\gamma = 120$	$\gamma = 120$	$\gamma = 120$					
CdO	$Fm\bar{3}m$	a = 4.6948	a = 4.7758	a = 4.7083	− 258.4	− 207.8	− 211.4	54.81	60.21
$\text{Mn}(\text{OH})_2$	$P\bar{3}m1$	a = 3.322	a = 3.3496	a = 3.2991	− 695.4	− 529.2	− 522.7	99.2	86.15
		c = 4.734	c = 4.7417	c = 4.5419					
		$\gamma = 120$	$\gamma = 120$	$\gamma = 120$					
$\text{Ni}(\text{OH})_2$	$P\bar{3}m1$	a = 3.13	a = 3.1665	a = 3.1203	− 529.7	− 381.9	− 397.8	88.0	70.42
		c = 4.63	c = 4.5814	c = 4.3581					
		$\gamma = 120$	$\gamma = 120$	$\gamma = 120$					
$\text{Zn}(\text{OH})_2$	$P\bar{3}m1$	a = 3.194	a = 3.2389	a = 3.1901	− 641.9	− 540.6	− 561.3	81.2	82.59
		c = 4.714	c = 4.6598	c = 4.4824					
		$\gamma = 120$	$\gamma = 120$	$\gamma = 120$					
$\text{Cd}(\text{OH})_2$	$I1m1$	a = 5.688	a = 5.7868	a = 5.6959	− 560.7	− 497.4	− 513.6	96.0	93.45
		b = 10.28	b = 10.2725	b = 10.0532					
		c = 3.42	c = 3.4943	c = 3.4321					
		$\beta = 91.4$	$\beta = 88.889$	$\beta = 88.548$					

Figure 1: Partial results of DFT calculations.

Figure 2 shows results for the thermochemistry calculations. HSC CHEMISTRY is a chemical reaction and equilibrium software package that can be used to calculate reaction equilibrium based on correlation of experimental data. Relatively large differences were observed between the calculated enthalpies of reaction at 298.15 K from all DFT methods and the experimentally measured values. PBEsol functional performs much better on average. Reaction entropies lie in between the HSC values (in the parenthesis) and the experimental data for the Mn-containing reactions.

Reaction	ΔH^0 Expt. ^a	ΔH_{PW91}	ΔH_{PBE}	ΔH_{PBEsol}	ΔH_{TPSS}	$\Delta H_{\text{revTPSS}}$	ΔH HSC ^c	ΔS^0 Expt. ^d	ΔS Calc. ^e
MnO + CO ₂ \rightleftharpoons MnCO ₃	-115.4	-77.71	-70.27	-100.85	-95.35	-117.65	-102.77	-187.71 (-167.83)	-176.29
NiO + CO ₂ \rightleftharpoons NiCO ₃	-70.18	-52.57	-65.89	-81.27	-112.80	-141.90	-63.05	-166.39	-194.78
ZnO + CO ₂ \rightleftharpoons ZnCO ₃	-68.8	-29.63	-36.33	-67.83	-108.59	-147.30	-68.76	-175.04	-174.01
CdO + CO ₂ \rightleftharpoons CdCO ₃	-98.73	-81.50	-78.91	-105.47	-117.64	-138.89	-99.36	-176.11	-173.77
Mn(OH) ₂ + CO ₂ \rightleftharpoons MnCO ₃ + H ₂ O	-47.0	-21.74	-16.98	-45.57	-55.70	-75.52	-33.88	-38.4 (-18.53)	-23.41
Ni(OH) ₂ + CO ₂ \rightleftharpoons NiCO ₃ + H ₂ O	-21.98	-1.53	-22.26	-27.72	-91.57	-121.63	-14.92	-27.6	-22.40
Zn(OH) ₂ + CO ₂ \rightleftharpoons ZnCO ₃ + H ₂ O	-19.2	-5.96	-17.88	-30.98	-90.23	-121.25	-19.18	-23.8	-22.24
Cd(OH) ₂ + CO ₂ \rightleftharpoons CdCO ₃ + H ₂ O	-38.2	-19.11	-11.29	-39.36	-50.29	-64.39	-38.69	-28.5	-17.97

^aAll the experimental values are computed from data in Table I at 298.15 K.

^bEnthalpies calculated with different functionals at 298.15 K including finite temperature phonon contributions.

^cValues taken from HSC database, at 303.15 K.

^dExperimental values are computed from data in Table I, at 298.15 K; values in the parenthesis are taken from HSC database at 303.15 K.

^eCalculated with the PW91 functional via the frozen-phonon method at 300 K.

Figure 2: Results of thermochemistry calculations.

5 Critical Review